



HAL
open science

The PPP code - User Manual -

Annette Calisti, Sandrine Ferri, Caroline Mossé, Bernard Talin

► **To cite this version:**

Annette Calisti, Sandrine Ferri, Caroline Mossé, Bernard Talin. The PPP code - User Manual -. PIIM physique des interactions ioniques et moléculaires; Aix Marseille Université; CNRS - Centre National de la Recherche Scientifique. 2024. hal-04501367

HAL Id: hal-04501367

<https://hal.science/hal-04501367>

Submitted on 12 Mar 2024

HAL is a multi-disciplinary open access archive for the deposit and dissemination of scientific research documents, whether they are published or not. The documents may come from teaching and research institutions in France or abroad, or from public or private research centers.

L'archive ouverte pluridisciplinaire **HAL**, est destinée au dépôt et à la diffusion de documents scientifiques de niveau recherche, publiés ou non, émanant des établissements d'enseignement et de recherche français ou étrangers, des laboratoires publics ou privés.

THE PPP CODE - USER MANUAL - MARCH 2024

A. CALISTI, S. FERRI, C. MOSSÉ, B. TALIN

1. INTRODUCTION - GENERAL CONSIDERATIONS.

The study of line shape is part of a set of complementary disciplines for the analysis of spectra, such as the study of atomic kinetics or the study of the hydrodynamic evolution of the medium. In plasmas, the Stark broadening of spectral lines results from the interaction of the emitter's internal degrees of freedom with the ionic and electronic micro-fields created by the plasma. Modeling this broadening is a complex problem involving a complex combination of atomic physics, statistical physics and plasma physics, the most challenging problem being to completely and correctly identify the emitter environment.

In particular, taking into account fluctuations in the electric fields produced on the emitter by moving ions and electrons has been of constant interest since the 1960s. Except for some specific cases, the calculation of line profiles in plasmas requires the use of numerical codes. There are a number of such codes of varying complexity, which necessarily differ in their field of application and accuracy. Among these codes, numerical simulation has played an increasingly important and unique role. In numerical simulations, we solve the Schrödinger equation describing the time evolution of the emitter's wave functions in the presence of a time-dependent electric field, then average it over a statistically representative set of electric fields. The simulation results are used as data of ideal experiments, but unfortunately this technique is very time-consuming and therefore limited to small atomic systems.

To circumvent this problem, approximate models have been developed that reproduce simulated profiles, i.e. taking charge correlations and charge movements into account, while enabling the study of complex emitters. In this context, we have developed the Frequency Fluctuation Model (FFM)^{1,2}, which is the basis of a fast and accurate calculation code (PPP code)³ designed to synthesize spectral profiles for the interpretation of experiments for a very wide range of emitters and plasma conditions.

Date: March 11, 2024.

¹B. Talin, A. Calisti, L. Godbert, R. Stamm, R.W. Lee et L. Klein, Frequency fluctuation Model for line-shape calculations in Plasma Spectroscopy, Phys. Rev. A 51,1918 (1995).

²A. Calisti, C. Mossé, S. Ferri, B. Talin, F. Rosmej, L.A. Bureyeva, V.S. Lisitsa, Dynamic Stark Broadening as The Dicke Narrowing Effect, Phys. Rev. E 81, 016406 (2010).

³A. Calisti, F. Khelifaoui, R. Stamm, B. Talin et R.W. Lee, Model for the line shape of complex ions in hot and dense plasmas, Phys. Rev. A 42, 5433 (1990).

For a long time, the PPP code had a special status because it had only a few international equivalents. One such code was the TOTAL code⁴, owned by LLNL and based on the primitive version of the PPP code we had developed in the 1990s. The second was the MERL code⁵ owned by the University of Florida, used and maintained by R. Mancini at the University of Nevada and a few years later, its optimized version, the MELS code⁶ has been developed at LLNL by C. Iglesias. Today, other codes have been developed to meet the need for interpretation of observations or synthetic diagnostics in magnetic or inertial confinement experiments, as well as in astrophysics. Among these codes, several have adopted the FFM in its new formulation (ref. 2) to deal with the problem of temporal fluctuations of plasma electric microfields^{7,8,9,10,11}.

A few general remarks about the code should be made:

First: In spite of the efforts intended to make the code friendly, lineshape calculations still remain difficult. Therefore, some knowledge about the atomic structure is necessary before starting a calculation. This is particularly useful for the adjustment of a few parameters that customize the code, with respect to both the capabilities of the computer and the algebra arising from the quantum calculation.

Second: The idea that codes can provide exact profiles should be given up. Besides the numerical traps, any lineshape calculation involves a series of necessary approximations. Thus, the most relevant strategy consists in, on the one hand, in choosing and carefully preparing the input data set needed for a sequence of calculations and, on the other hand, in checking the discrepancies of results as often as possible, by comparison with previous calculations or other available theoretical or experimental spectra. A lineshape calculation should be merely viewed as a converging process rather than as a straightforward analytical calculation.

⁴C.J. Keane, R.W. Lee, B.A. Hammel, A.L. Osterheld, L.J. Suter et A. Calisti, F. Khelifaoui, R. Stamm et B. Talin, *Rev. Sci. Instrum.* 61, 2780 (1990).

⁵R.C. Mancini et al., *Computational aspect of the Stark line broadening of multielectron ions in plasmas*, *Comput. Phys. Commun* 63, 314 (1991).

⁶C. A. Iglesias, *Efficient algorithms for stochastic Stark-profile calculations*, *High Energy Density Physics* 9, 209-221, (2013).

⁷E. Stambulchik and Y. Maron, *Quasicontiguous frequency-fluctuation model for calculation of hydrogen and hydrogenlike Stark-broadened line shapes in plasmas*, *Phys. Rev. E* 87, 053108 (2013).

⁸S. Alexiou, *Implementation of the Frequency Separation Technique in general lineshape codes*, *High Energy Density Physics* 9 (2013) 375-384.

⁹S. Lorenzen, B. Omar, M. C. Zammit, D. V. Fursa, I. Bray, *Plasma pressure broadening for few-electron emitters including strong electron collisions within a quantum-statistical theory*, *Phys. Rev. E* 89, 023106 (2014).

¹⁰E. G. Hill, G. Perez-Callejo, S.J. Rose, *ALICE : A non-LTE plasma atomic physics, kinetics and lineshape code*, *High Energy Density Physics*, Vol : 26, Pages : 56-67, (2018).

¹¹F. Gilleron, J.C. Pain, *ZEST : A Fast Code for Simulating Zeeman-Stark Line-Shape Functions*, *Atoms* 6(1), 11 (2018).

Third: In its present state the code has been carefully tested using different FORTRAN compilers. Nevertheless, remaining bugs or weaknesses could occasionally appear. The authors should appreciate any information and any suggestions about such encountered problems.

Fourth: This code results from a long and fruitful collaboration between France and USA. It has been funded by a contract between the University of California (LLNL) and the Aix-Marseille University (former Université de Provence) (purchase order B108505). On the American side, R. W. Lee projected the realization of the code and actively participated from the beginning to its development. The main work performed on the French side was due to A. Calisti, R. Stamm and B. Talin with the helpful collaboration of students and various collaborators.

Fifth: The code has continued to evolve and to be improved over time. The electronic collision operator has been improved to take into account interference terms. The code was rewritten in Fortran 90 to take advantage of dynamic array allocation. A new formulation of the FFM has simplified its use and saved computing time. A version of the code was written to account for both the Stark and Zeeman effects¹² (not described here).

Sixth: It is regularly compared with other codes and models as part of the Spectral line shapes in Plasma code comparison workshop organized every two years since 2012 in collaboration with IAEA¹³.

This manual is divided in two sections and three appendices: first, the theoretical background is explained. Then, examples and dumps of simple runs are used that show how the code works. Appendix A is devoted to a brief review of the Liouville space. Appendix B describes the electronic collision operator and Appendix C is devoted to the Markov process used in the FFM.

¹²S. Ferri, O. Peyrusse, A. Calisti, Matter Radiat. Extremes 7, 015901 (2022).

¹³<https://plasma-gate.weizmann.ac.il/slsp/>

2. THEORETICAL BACKGROUND.

2.1. Theoretical Preliminary.

The usual introduction of the theoretical point of view for lineshape, starts from the dipole auto correlation function $C(t)$ related to the radiation intensity through the Fourier transform:

$$(1) \quad I(\omega) = \frac{1}{\pi} \Re \int_0^\infty C(t) e^{i\omega t} dt$$

where, in Liouville space notation, $C(t)$ is given by the trace:

$$(2) \quad C(t) = \ll \vec{d}^* | U(t) | \rho_0 \cdot \vec{d} \gg .$$

d and ρ_0 are respectively the dipole and the equilibrium density matrix operator for finite quantum systems (a brief review of Liouville space formalism is given in appendix A). $U(t)$ is an average evolution operator for the quantum emitter system, it is the solution of a stochastic equation of the form¹⁴.

$$(3) \quad \begin{aligned} \frac{dU_f(t)}{dt} &= i(L_0 + l_f)U_f(t) \\ U_f(0) &= 1 \end{aligned}$$

l_f is a time-dependent Liouville perturbation operator which connects the quantum emitter system to an external electric field f . f represents a time-dependent perturbation history and belongs to a functional measurable space $\{F, P\}$ providing a way to calculate any average quantity by means of discrete weighted sums, or a more general integration process, with a given measure or a probability density

$$(4) \quad U(t) = \langle U_f(t) \rangle_f .$$

The resolution of the above stochastic equation is a two step process: the resolution of the Liouville equation for the field histories is followed by an integration over the functional space. It should be noted that the line shape problem is simpler than the resolution of the stochastic Liouville equation (SLE) itself because the quantum average in trace (Eq. 2) works as a filter that erodes the complete information involved in $U(t)$. So, as far as the final purpose is limited to the calculation of line shapes, it is worthwhile to develop methods that take advantage of this simplification. The SLE has at least two well known limits. The first one is the impact limit that corresponds to binary collisional events between emitters and the perturber bath. For this case, the mean time between collisions is much longer than the collision time itself. The second one is the static limit for which, the functional space is well characterized by a probability density of external fields. For both these limits, solutions of the SLE exist. For intermediate cases, that is, non-impact and non-static cases, the SLE must be solved for emitters perturbed by a fluctuating electric field. In addition, electrons faster than ions, give rise to a smooth decorrelation mechanism of the radiation generally represented in the SLE by a collision operator. A model for an electron collision operator is proposed in appendix B.

¹⁴N. Van Kampen, Stochastic Processes in Physics and Chemistry (North-Holland, Amsterdam 1981)

Accounting for the fluctuations of electric fields produced at emitters, by moving electrons and ions, has been of constant interest for both the experimental and theoretical points of view since the 1960s¹⁵.

Different methods have been developed among which the model micro field method MMM¹⁶, numerical simulations^{17,18,19,20,21} and kinetic theory models such as those developed by Boerker, Iglesias and Dufty (BID)²² and frequency fluctuation model (FFM)²³ have proven to be the most successful. Recently, with the advances in computer technology, two-component ion plus electron plasma molecular dynamics (MD) simulations have been applied in studies devoted to spectral line shapes^{24,25,26}.

2.2. Static Stark component calculations.

In the PPP code, the average over the plasma perturbers in Eq. 2 is performed in two steps. The electron component is assumed to interact with the emitter through binary collisions. The whole effect of the electrons may then be represented by an electronic collision operator of the type described in the Appendix B²⁷. This electronic collision operator constitutes the main part of the homogeneous broadening mechanism. A second step consists of an average over the ions screened by the electrons. This average over the ions, together with the Doppler broadening, constitute the inhomogeneous part of the broadening. The quasistatic ion approximation which has been used leads to an average over a microfield distribution function $P(f)$. Methods for the calculation of the microfield distribution valid for all conditions from weakly to strongly coupled plasmas have been chosen^{28,29}.

Our model leads to the following form of the evolution operator $U_f(t)$, averaged over the electrons in a constant ion field f :

$$(5) \quad U_f(t) = e^{-i(L_f - i\Phi)t},$$

where L_f , is the Liouville operator of the quantum system of interest, perturbed by a static external electric field f . The diagonal elements of this operator are atomic frequencies and the non-diagonal terms the Stark interaction terms. The non-Hermitian

¹⁵H.Griem, Principles of Plasma Spectroscopy, Cambridge University Press, Cambridge,1997.

¹⁶A. Brissaud and U. Frisch, J. Quant. Spectrosc. Radiat. Transf. 11, 1167 1971; J. Math. Phys. 15, 524 1974.

¹⁷R. Stamm et al., Phys. Rev. A 30, 2039 1984.

¹⁸R. Stamm, B. Talin, E. L. Pollock, and C. A. Iglesias, Phys. Rev. A 34, 4144 1986.

¹⁹J. Seidel, Spectral Line Shapes Deepack, Hampton, VA, 1987, Vol. 4, p. 57.

²⁰G. C. Hegerfeldt and V. Kesting, Phys. Rev. A 37, 1488 1988.

²¹V. Cardenoso and M. A. Gigosos, Phys. Rev. A 39, 5258 1989.

²²D. B. Boercker, C. A. Iglesias and J. W. Dufty, Phys. Rev. A 36, 2254 1987.

²³B. Talin, et al., Phys. Rev. A 51,1918 (1995).

²⁴E. Stambulchik, et al., High Energy Density Phys. 3, 272 2007.

²⁵M. Gigosos et al., Phys. Rev. E 98, 033307 2018.

²⁶A. Calisti et al., High Energy Density Phys. 50, 101084 2024.

²⁷Hans R. Griem, Milan Blaha, and Paul C. Kepple, Phys. Rev. A 19, 2421 (1979).

²⁸C. A. Iglesias et al., Phys. Rev. A 28, 1667 (1983); Phys. Rev. A 31, 1698 (1985).

²⁹C. F. Hooper, Jr., Phys. Rev. 149, 177 (1966); 165, 21 (1968).

diagonal operator, Φ , represents all the homogeneous broadening effects, i.e., the electronic and natural broadening.

$C(t)$ can thus be written as:

$$(6) \quad C(t) = \int P(f) S_f(t) df$$

where

$$(7) \quad S_f(t) = \ll \vec{d}^* | U_f(t) | \vec{d} \rho_0 \gg .$$

The spectral intensity of the emitted radiation is proportional to the Laplace transform of S averaged over microfield states:

$$(8) \quad I(\omega) = \frac{1}{\pi} \Re \left[\int P(f) \int_0^\infty e^{i\omega t} S_f(t) dt df \right] .$$

The line shape results from a competition between in homogeneous and homogeneous broadening. Due to degeneracy removal, the Stark effect breaks each initial line into many Stark components on which natural and electronic relaxation act as a noise filter. This suggests the possibility of replacing the integral for the microfield average with a weighted sum over n_f terms:

$$(9) \quad I(\omega) = \sum_{f=1}^{n_f} P_f I_f(\omega) .$$

In this expression, $I_f(\omega)$ is the line-shape function for a fixed ion field with label f , and the data set P_f , is chosen in order to optimize computer time and accuracy for the final line profile.

At this point there are two paths which can be followed: Either we perform the Fourier transform and then invert the resulting matrix, or we explicitly express $e^{-i(L_f - i\Phi)t}$ and Fourier transform it. The latter path is preferred because it generally leads to large reductions in computer time. In order to follow this path, the basic idea is to look for the basis in which $L_f - i\Phi$ is diagonal. In such a basis, let us denote by $|k\rangle$ the eigenvectors of $L_f - i\Phi$, with complex eigenvalues z_k . If M_f , is the similarity transformation matrix, we may write the line-shape function in an electric microfield strength f by:

$$(10) \quad I_f(\omega) = \frac{1}{\pi} \Re \ll \vec{d}^* | M_f \int_0^\infty e^{i\omega t} e^{-iM_f^{-1}(L_f - i\Phi)M_f t} dt M_f^{-1} | \vec{d} \rho_0 \gg .$$

The Fourier transform in this expression is easily performed, leading to the following structure for I_f :

$$(11) \quad I_f(\omega) = \frac{1}{\pi} \Im m \ll \vec{d}^* | M_f \left(\begin{array}{ccc} \cdot & & \\ & \frac{1}{\omega - z_k} & \\ & & \cdot \end{array} \right) M_f^{-1} | \vec{d} \rho_0 \gg .$$

This expression can be written as:

$$(12) \quad I_f(\omega) = \sum_k \frac{c_k(\omega - \omega_k) + a_k\gamma_k}{(\omega - \omega_k)^2 + \gamma_k^2},$$

where the sum is over the eigenvalues of $L_f - i\Phi$ for a given field f .

The static profile is then described by a sum of rational fractions which are generalized Lorentzian spectral components of the line, i.e., the Stark spectral components or Stark dressed components, defined by two complex numbers, the generalized intensity $a_k + ic_k$ and the generalized frequency $z_k = \omega_k + i\gamma_k$.

Working in the space of the Stark dressed transitions (SDT), we can rewrite the linear response line-shape function in terms of dressed two-level radiators by defining a generalized dipole moment matrix element D_k for the SDT. The normalized matrix element is given by:

$$(13) \quad D_k = r \sqrt{1 + i \frac{c_k}{a_k}}$$

where $r = \sqrt{\sum a_k}$ is the reduced matrix element of the transition associated with the emission of the SDT. This generalized dipole moment matrix element can be considered to be the diagonal element of the k th component of a vector operator D , which acts in the extended Liouville space. We also define the probability vector operator p with element p_k describing the instantaneous probability of occurrence of the k th SDT. This probability is determined by the normalized real part of the amplitude or relative intensity of the SDT:

$$(14) \quad p_k = \frac{a_k}{r^2}.$$

The spectral line shape in the quasi static approximation is then given by in the basis of the SDT:

$$(15) \quad I(\omega) = \frac{1}{\pi} \Re \sum_{k,j} i \ll D_k | (\omega \mathbf{1} - L_0)^{-1} | D_j \gg p_j,$$

where the Liouville operator L_0 has a set of eigenfrequencies, $\omega_k + i\gamma_k$, composed of the generalized frequencies and widths of the SDT.

The Liouville space matrix element of the propagator is a trace over the SDT states, which include the emitter-plasma interaction. The ion microfield is considered to be quasistatic at this point, so that, in this approximation, the propagator is diagonal in the SDT index and the line shape is a sum of independent contributions from a set of generalized Lorentzian terms. Each independent term in this sum is to be associated with the emission from one of the n SDT that interact with the radiation field through the generalized dipole moment D . The next step is to extend this formulation to include ion dynamics, i.e., the time-dependent effect of a fluctuating ion microfield on the spectral line shape.

2.3. Field Fluctuation and Frequency Fluctuation Models.

If the microfield is time varying, the SDT are subject to a collision-type mixing process (a Markov process) induced by the field fluctuations.

The chosen Markov process is completely determined by two sets of quantities: the instantaneous SDT probability operator p , with elements defined in Eq. 14, and a transition rate operator \mathbf{W} such as:

$$(16) \quad \mathbf{W}_{kj} = -\Gamma_j \delta_{kj} + W_{kj}.$$

The linear-response line shape resulting from the stochastic mixing of the radiation channels can be written in the Liouville space of the SDT and is then given by ³⁰:

$$(17) \quad I(\omega) = \frac{1}{\pi} \Re \sum_{k,j} i \ll D_k | (\omega \mathbf{1} - L_0 + i\mathbf{W})^{-1} | \mathbf{D}_j \gg \mathbf{p}_j.$$

Thus:

$$(18) \quad I(\omega) = \frac{1}{\pi} \Re \sum_{k,j} i \ll D_k | (\omega \mathbf{1} - L_0 - i\Gamma + iW)^{-1} | D_j \gg p_j.$$

Γ is the diagonal matrix of inverse state lifetimes with $\Gamma_{kj} = \nu \delta_{kj}$ and W is the matrix of transition rates between different states such as $W_{kj} = \nu p_k$.

Defining the quasistatic propagator:

$$(19) \quad G^s(\omega) = (\omega \mathbf{1} - L_0 - i\Gamma)^{-1}$$

which has only diagonal matrix elements, the total propagator $G(\omega)$, can be written as:

$$(20) \quad G(\omega) = G^s(\omega) - iG^s(\omega) \cdot W \cdot G(\omega).$$

Introducing this expression in Eq. 18 and ignoring the homogeneous width to lighten the equations, we get:

$$(21) \quad [1 \cdots 1] G(\omega) \begin{bmatrix} a_1 \\ \vdots \\ a_n \end{bmatrix} = [1 \cdots 1] G^s(\omega) \begin{bmatrix} a_1 \\ \vdots \\ a_n \end{bmatrix} - i [1 \cdots 1] G^s(\omega) \cdot W \cdot G(\omega) \begin{bmatrix} a_1 \\ \vdots \\ a_n \end{bmatrix}$$

The W matrix taking the following form, due to the sum rules,

$$(22) \quad W = \begin{bmatrix} \nu \frac{a_1}{r^2} & \cdots & \nu \frac{a_1}{r^2} \\ \vdots & & \vdots \\ \nu \frac{a_n}{r^2} & \cdots & \nu \frac{a_n}{r^2} \end{bmatrix} = \frac{\nu}{r^2} \begin{bmatrix} a_1 \\ \vdots \\ a_n \end{bmatrix} [1 \cdots 1]$$

³⁰A. Calisti et al., Phys. Rev. E 81, 016406 (2010).

we get:

$$(23) \quad [1 \cdots 1] G(\omega) \begin{bmatrix} a_1 \\ \vdots \\ a_n \end{bmatrix} = [1 \cdots 1] G^s(\omega) \begin{bmatrix} a_1 \\ \vdots \\ a_n \end{bmatrix} - i \frac{\nu}{r^2} [1 \cdots 1] G^s(\omega) \begin{bmatrix} a_1 \\ \vdots \\ a_n \end{bmatrix} [1 \cdots 1] G(\omega) \begin{bmatrix} a_1 \\ \vdots \\ a_n \end{bmatrix}$$

This gives rise to the equation:

$$(24) \quad \sum_{kj} \langle 1 | G(\omega) | D_k p_k \rangle = \sum_k \frac{a_k}{\omega - \omega_k - i\nu} - i \frac{\nu}{r^2} \sum_k \frac{a_k}{\omega - \omega_k - i\nu} \times \sum_{kj} \langle 1 | G(\omega) | D_k p_k \rangle$$

and,

$$(25) \quad \sum_{kj} \langle 1 | G(\omega) | D_k p_k \rangle = \frac{\sum_k \frac{a_k}{\omega - \omega_k - i\nu}}{1 + i\nu \sum_k \frac{a_k/r^2}{\omega - \omega_k - i\nu}}$$

Finally, the line profile is given by:

$$(26) \quad I(\omega) = \frac{r^2}{\pi} \text{Re} \frac{\sum_k \frac{a_k/r^2}{i(\omega - \omega_k) + \nu}}{1 - \nu \sum_k \frac{a_k/r^2}{i(\omega - \omega_k) + \nu}}$$

All the above results are easily extended to the continuous case. In this case, the probability $p_k = \frac{a_k}{r^2}$ is replaced by $W(\omega)d\omega$ the probability to have a radiation at a frequency in the range ω and $\omega + d\omega$ obtained in the static limit. The previous equation is then written as:

$$(27) \quad I(\omega) = \frac{r^2}{\pi} \text{Re} \frac{\int \frac{W(\omega')d\omega'}{\nu + i(\omega - \omega')}}{1 - \nu \int \frac{W(\omega')d\omega'}{\nu + i(\omega - \omega')}}.$$

With $W(\omega)$ being the normalized static line shape.

We thus obtain an expression of the dynamic line profile as a functional of the static frequency distribution and a unique parameter, the fluctuation rate. The main numerical work is the calculation of this static profile.

2.4. Summary Through a Short Example.

The previous discussion about the frequency fluctuation model can be illustrated considering a very simple academic example: the hydrogenic Lyman alpha line, without fine structure, imbedded into a stochastic electric field.

The relevant atomic states in the nlm representation are:

$$|1, 0, 0 \rangle, |2, 0, 0 \rangle, |2, 1, -1 \rangle, |2, 1, 0 \rangle, |2, 1, 1 \rangle$$

respectively noted 1 to 5. The quantum axis has been chosen in the supposed direction z of the external static field. Therefore, due to the dipole selection rules, when an electric field is applied, only the states 2 and 4 are coupled together. The resulting

spectrum shows a central component associated with the states 3 and 5 and two lateral components related to both the new non-degenerated Stark states built upon the states 2 and 3. The fluctuations of the field magnitude induce a frequency fluctuation while the changes in direction modify the projection of the Stark states on the excited state basis. When a field jump occurs, a redistribution of the frequency spectrum among the various components, including the un-shifted central one, takes place. These dynamic events, as previously discussed, induce both a broadening of the central component and a coalescence of the whole spectrum towards the central frequency insuring that the fast fluctuation limit gives the un-perturbed spectrum. The main step is devoted to find the eigen energies of the evolution operator for each electric field value. Then, these data are mixed up using a simple Markov process providing a new data set available for the final line shape calculation.

3. CODE DESCRIPTION

3.1. Overview.

The code has been divided into three parts that respectively prepare, process and build the spectra.

The main motivation maintaining the code PPP into three pieces has been to make the work of the three independent tasks easier on small computers. These three tasks are:

- **pim**: sets the necessary links with the external data bases and the output files and the plasma parameters. It also selects the relevant quantum systems.
- **pam**: processes the hard algebra stage
- **poum**: carries out the final calculation of lineshapes according to particular options and formats.

The first phase **pim** can be viewed as a dialog with the code which helps the user to extract a well-shaped data subset from the atomic database according to both the constraints of computer time-saving and appropriate selection of the relevant couplings for Stark effect calculations. Therefore, the first phase could be run many times before starting the hard subsequent phase in order to improve the system selection.

The algebra involved in the second phase **pam** is basically a sequence of quantum mechanical calculations of the same trace necessary to account for the average on the microfield distribution. Most of the computer time is spent with this phase which has been designed with particular care to save computer time. The first step in this phase deals with the filling, for one external electric field q , of the relevant matrices involved in the trace:

$$(28) \quad \ll \vec{d}^t | U_q(t) | \rho_0 \cdot \vec{d} \gg .$$

Once the symmetry properties of the evolution operator have been found, the eigenenergies as well as the corresponding unitary transformations are derived:

$$(29) \quad \ll \vec{d}^t M_q | e^{iZ_q t} | M_q^{-1} \rho_0 \cdot \vec{d} \gg .$$

The numerical difficulty here lies in the diagonalization of complex matrices. Complex matrix diagonalization is a nontrivial problem that can be the most severe and the most limiting part of the calculation. Finally, instead of calculating the trace, the characteristic complex coefficients of the Stark components are picked up and stored to be processed by the third phase:

$$(30) \quad \begin{aligned} f_{qi} + i\gamma_{qi} &= (Z_q)_{ii} \\ a_{qi} + ic_{qi} &= (\vec{d}^t M_q)_{ii} \cdot (M_q^{-1} \rho_0 \vec{d})_{ii}. \end{aligned}$$

The third phase **poum** is the simplest one. It just includes sums of elementary Lorentzian profiles defined with the above parameters and, if necessary, convolutions.

These three phases and the main algorithms used in some key steps will be described below. This description is preceded by indications about the way to compile the PPP code.

3.2. Compilation of the Code: Phase 0.

The PPP code, `ppp.f90`, is written in Fortran 90. It calls on several library subroutines (`lapack77` and `lapack90`) located in three external files: `interf_cggeevsv.f90`, `hnclib_w4.f90`, `libgeevsv.for`.

To create an executable program, it is first necessary to compile suppressing the link edit phase, the three external files. Then, the PPP program will be compiled and linked with the three object files created previously.

For example, by using the Intel fortran in an UNIX environment:

```
>> ifort -c interf_cggeevsv.f90
>> ifort -c hnclib_w4.f90
>> ifort -c libgeevsv.for
```

The `-c` option suppresses the link-edit phase. The compiler generates an object file with the extension `.o` for each input file.

Then, the compilation of `ppp.f90` will be performed by:

```
>> ifort -o PPP ppp.f90 interf_cggeevsv.o hnclib_w4.o libgeevsv.o
```

The `-o PPP` option causes the compiler to name the output file PPP instead of `a.out`. The PPP code is now ready to be run.

```
>> ./PPP
```

When the code is run for the first time, a set of default variables appears on the screen in a dialog window with the user. The Pim: Data Pre-processing is starting.

3.3. Pim: Data Pre-processing - Phase 1.

The task devoted to `pim` is to make available for the second phase `pam` the whole data set needed for a calculation, that is: a) the coefficients that define the plasma characteristics and the bounds of the frequency window, b) the field statistical properties and c) the atomic data for the quantum calculation. When the first step is done with the help of a friendly interactive routine, `pim` starts reading, selecting and processing the data to be written down into the files `miscel` and `samfld` embodying coefficients, atomic data and statistical information about the micro field for the given problem.

3.3.1. Pim: Plasma Condition Input.

If "PPP" is run for the first time, a default set of variables is typed into the screen and the default file `in_new.txt` is created in the user's directory. Subsequent executions systematically reopen the modified file `in_new.txt` and ask to choose whether to execute "pim", "pam", or "pum".

| | | | default set of variables |
|----|-------------------|-------------|---|
| 1 | Ar17.dat | **** | (base,pfi) atom data base/ pop file |
| 2 | 3300.00 | 3340.00 | (da, db) frequency interval bounds - eV |
| 3 | 40.000 | 1.000 | (em, pm) emitter/ perturber mass |
| 4 | 17.000 | 1.000 | (ze,zp) net emit. charge/ pert. charge |
| 5 | 0.10000E+08 | 0.10000E+08 | (tmpe, tmpi) electron temp/ ion temp. - K |
| 6 | 0.10000E+25 | 0.10000E-01 | (dens,per) elec dens/ emit/pert concent |
| 7 | 2. | 10. | (lay,set) layer b/ stark trans cutoff |
| 8 | 2 | | (nu) block rad trans nb |
| 9 | outd | outs | (out, sdof) Stark data, output file |
| 10 | n | | (ric) interference terms (y/n) |
| 11 | 50 | 25. | (nmc, ecut) fld number/ max field value |
| 12 | new data? or help | | |

To modify this file and enter a new data one can simply write `variablename=new data` without space character (note that `in_new.txt` can also be edited). Most of these data have a straightforward significance. For the others, it will become clearer later.

base: Atomic database filename : maximum character number = 12. The databases must generally be provided by known atomic physic codes (MCDF Grant's code, Cowan's code, FAC code, HULAC, SUPERSTRUCTURE...) and written with a format that can be read by the PPP code.

pfi: Optional level population filename.

lay, xset: The parameters lay and xset whose role will be developed in the next section are used to monitor the quantum system configuration.

nu: Sets the number of radiative transitions which can be processed at a time. That means that one can either process n small quantum systems for n radiative transitions or about n/nu bigger ones for the same case.

out: Output filename for the Stark component data, to be post-processed by pum

sdof: Output filename for the profiles.

ric: By default, ric=n. If the ric=y option is choosen, interference terms are accounted for in the calculation of the profile.

nmc: Gives the number of significant points for the micro field distribution. Twice as many of these points doubles the calculation time. Indeed, this number that defines a more or less coarse distribution, provides a way to monitor the final result. This is a matter of optimization.

ecut: Maximum field values of the microfield distribution by default, ecut=25. In some cases, ecut must be increased.

The atomic database must be in the user's directory when the PPP code is executed. If this is not the case, the following message appears on the screen.

```
check if atomic database is in your folder
```

The default `in_new.txt` file is created in the user directory. It contains the previous default file and the default variables used by "pum". The latter are described in the section dedicated to `pum`.

| | | in_new.txt | |
|----|-------------|-------------|--|
| 1 | Ar17.dat | **** | (base,pfi) atom data base/ pop file |
| 2 | 3300.00 | 3340.00 | (da, db) frequency interval bounds - eV |
| 3 | 40.000 | 1.000 | (em, pm) emitter/ perturber mass |
| 4 | 17.000 | 1.000 | (ze,zp) net emit. charge/ pert. charge |
| 5 | 0.10000E+08 | 0.10000E+08 | (tmpe, tmpi) electron temp/ ion temp. - K |
| 6 | 0.10000E+25 | 0.10000E-01 | (dens,per) elec dens/ emit/pert concent |
| 7 | 2. | 10. | (lay,set) layer b/ stark trans cutoff |
| 8 | 2 | | (nu) block rad trans nb |
| 9 | outd | outs | (out, sdof) Stark data, output file |
| 10 | n | | (ric) interference terms (y/n) |
| 11 | 50 | 25. | (nmc, ecut) fld number/ max field value |
| 12 | e | 300 | (units,npt)(e/a)eV or A/curve point numb. |
| 13 | 3300.00 | 3340.00 | (ai,af) default frequency range |
| 14 | n | f | (dop,cv)doppler (y/n)-convol(f)fft(v)voigt |
| 15 | 0.00000 | 0.00000 | (wg,wl) Gauss FWHM/ Lorentz HWHM eV |
| 16 | n | | (nyn) profile normalization y/n |
| 17 | 0.00000 | | (shft) shift in output units |

3.3.2. *Pim: Statistical Data Input.*

For the next step the user may optionally direct the code to process a micro field distribution function, answering the question with "y" or an appropriate filename. If such a distribution has already been calculated or if a one-field case is considered, a carriage return skips this step

m-field calculation y(es) (no def.)
or filename (other distribution)

A filename input instead of "y" requires the code to read this file and to process a file `samfld.dat` with the correct format for `pam`. This should be useful for instance to run the code with a simulated distribution or any other suitable function. In the standard case, when $ze \neq 0.$, the microfield distribution is obtained running the `apex` routine³¹ that permits the plasma microfield to be calculated for any conditions in both weakly and strongly coupled plasmas. Due to the well proven accuracy of the `apex` results, this part of the code can be considered as a problem solved which frees theorists to concentrate on other areas. When $ze=0.$, the microfield distribution is obtained running the `hooper` routine³².

The code processes the data provided by `apex` (or one other function) in order to interpolate the required number `nmc` of significant probabilities on points regularly displayed

³¹C. A. Iglesias et al., Phys. Rev. A 28, 1667 (1983); Phys. Rev. A 31, 1698 (1985).

³²C. F. Hooper, Jr., Phys. Rev. 149, 177 (1966); 165, 21 (1968).

on the distribution function. The "field" file, which contains the raw distribution resulting from the calculation before the processing required for a "pam" calculation, is also written to the user directory.

3.3.3. Pim: Atomic System Selection.

The automatic selection of a quantum system for a given problem is a nontrivial optimization process. Many constraints must be considered at a time.

- the bigger the system is, the better the Stark effect is accounted for.
- the smaller the system is, the faster the calculations are.
- big systems could deal with numerical traps.

The selection algorithms work finding the successive neighbors of a radiative transition. The first neighbors are selected using the mean Stark shift but the following ones are characterized by the blending ratios due to Stark couplings. More precisely, the estimated coupling strength u of a state b on a state a , through the intermediate states i_1, i_2, \dots, i_n , is given with the product:

$$(31) \quad u(a, b) = s(a, i_1) \times m(i_1, i_2) \times \dots \times m(i_n, b)$$

where s gives the Stark shift and m the blending ratios between two adjacent states. That is, the eigen-state coefficients in the non perturbed basis. For two degenerated states i and j , we simply have $m(i, j) = (1/2)^{1/2}$. This is the maximum contribution for neighbors beyond the first ones. The mean electric field enters into the calculation of the mean Stark shift that thus depends on the electronic density. Therefore, the selected quantum systems can vary with the plasma conditions. The algorithm uses three coefficients previously mentioned for selecting the quantum system:

lay: number of successive neighbor shells to be considered.

nu: number of radiative transitions that can be processed at a time.

xset: minimum relative strength of a state taken into account. If q is the larger Stark shift induced by the first neighbors, one must have :

$$(32) \quad u(a, b) = \frac{q}{xset}.$$

The selection process is complemented by the possible cancellation by means of an interactive dialog at the keyboard, of each radiative transition. This is useful for simplification purposes or to study the contribution of a particular transition to a spectroscopic pattern. Finally, **pim** writes the second file needed for the following phase **pam** whose name is **miscel..** Two simple examples of the **miscel..** files are given below:

| miscel. | | | |
|---------|-------------|-------------|--|
| 1 | Ar17.dat | **** | (base,pfi) atom data base/ pop file |
| 2 | 3300.00 | 3340.00 | (da,db) frequency interval bounds - eV |
| 3 | 40.000 | 1.0000 | (em,pm) emitter/ perturber mass |
| 4 | 17.000 | 1.0000 | (ze,zp) net emit. charge/ pert. charge |
| 5 | 0.10000E+08 | 0.10000E+08 | (tmpe,tmpi) electron temp/ ion temp. - K |

```

6  0.10000E+25  0.10000E-01  (dens,per) elec dens/ emit/pert concent
7  2  10.  (lay,xset) layer nb/ stark trans cutoff
8  2  (nu) block rad trans nb
9  outd  outs  (out,sdof)Stark data, output file
10 n  (ric) interference terms (y/n)
11 50 25.  (nmc,ecut) fld number/ max field value
12 e 300  (units,npt)(e/a)eV or A/curve point numb.
13 3300.00 3340.00  (ai,af) default frequency range
14 n f  (dop,cv)doppler(y/n)-convol(f)fft(v)voigt
15 0.00000 0.00000  (wg,wl) Gauss FWHM/ Lorentz HWHM eV
16 n  (nyn) profile normalization y/n
17 0.00000  (shft) shift in output units
18 2.937  (t) fluctuation rate
19 2  (krad) radiative transition number
20 1 4 4  (levg,lev,ltrs) ground level,total level & trans. number
21 lab. /name /energy /spont. /popu. /2j+1 / /n
22 1 ss1s00 0.000000 0.00000E+00 0.10000E+01 2 1
23 2 pp2p01 3318.220703 0.42603E-01 0.21268E-01 2 2
24 3 ss2s00 3318.388428 0.90349E-13 0.21264E-01 2 2
25 4 pp2p00 3323.036377 0.43184E-01 0.42299E-01 4 2
26 i-lab. /j-lab. /redu. / /dlambda /xstrs
27 1 2 -0.57735E-01 0.37366E+01 0.39595E-03 2
28 2 3 -0.23400E+00 0.73932E+05 0.45626E+01 1
29 1 4 -0.82023E-01 0.37311E+01 0.79800E-03 2
30 3 4 -0.33237E+00 0.26675E+04 0.46720E+01 1

```

In addition to the header that corresponds to the file `in_new.txt` modified by `pim`, the code writes an estimate of the fluctuation rate for the Markovian fluctuation model and four integers corresponding respectively to:

t: the frequency fluctuation rate to be used in the FFM procedure

krad: number of radiative transitions actually considered

levg: number of ground levels

lev: total number of levels

ltrs: total number of transitions

The remaining part of the file embodies the atomic data for the problem, that is successively, the level data package and the transition data package. In the first package, the only relevant data used by the main processing are:

```
lab. /energy /popu. /2j+1 / /n
```

Let's say, the level's identification label, its energy, its occupancy probability (default, at ETL), $2j+1$ (the number of m_j values for a given value, j , of the level's total angular momentum) and the principal quantum number.

In the second one, only the first three columns and the last one are used. The third is filled with the reduced matrix elements needed for the evaluation of the dipole matrix with the Wigner-Eckart theorem. The last column identifies and stores radiative transitions (marked 2) and Stark couplings (marked 1). The other data are written for convenience.

If the `nu` is set to 1 then the two following blocks are obtained in `miscel.`:

```

1                                     miscel.
2      1  4  3  (levg,lev,ltrs) ground level,total level & trans. number
3      lab. /name /energy /spont. /popu. /2j+1 / /n
4      1    ss1s00      0.000000  0.00000E+00  0.10000E+01  2  1
5      2    pp2p01     3318.220703  0.42603E-01  0.21268E-01  2  2
6      3    ss2s00     3318.388428  0.90349E-13  0.21264E-01  2  2
7      4    pp2p00     3323.036377  0.43184E-01  0.42299E-01  4  2
8      i-lab. /j-lab. /redu. / /dlambda /xstrs
9      2    3    -0.23400E+00  0.73932E+05  0.45626E+01  1
10     1    4    -0.82023E-01  0.37311E+01  0.79800E-03  2
11     3    4    -0.33237E+00  0.26675E+04  0.46720E+01  1
12     1  4  3  (levg,lev,ltrs) ground level,total level & trans. number
13     lab. /name /energy /spont. /popu. /2j+1 / /n
14     1    ss1s00      0.000000  0.00000E+00  0.10000E+01  2  1
15     2    pp2p01     3318.220703  0.42603E-01  0.21268E-01  2  2
16     3    ss2s00     3318.388428  0.90349E-13  0.21264E-01  2  2
17     4    pp2p00     3323.036377  0.43184E-01  0.42299E-01  4  2
18     i-lab. /j-lab. /redu. / /dlambda /xstrs
19     1    2    -0.57735E-01  0.37366E+01  0.39595E-03  2
20     2    3    -0.23400E+00  0.73932E+05  0.45626E+01  1
21     3    4    -0.33237E+00  0.26675E+04  0.46720E+01  1

```

that will give rise for `pam` to a stepwise calculation, one for each radiative transition. The various blocks correspond to separate quantum systems.

A file, `bars`, containing the energies and intensities of the radiative transitions selected by `pim` is also written in the user directory for convenience.

When `pim` is run, the user is asked a number of questions. In particular, at the end of the run, the user is asked whether or not he/she wishes to consult the `miscel.` file. It is advisable to do so until you are sure you have optimized the atomic system to be processed by "pam". If you stop execution to consult `miscel.`, when PPP is restarted, the user is asked whether to execute `pim`, `pam` or `pum`. At this stage, answer `pam` to continue the calculation or `pim` to modify the atomic data selection. If you don't consult `miscel.`, the program goes straight to executing `pam`.

3.4. Pam: Data Processing: Phase 2.

This phase begins with:

| | | | | |
|---|--------------------------------|-------------------|--------------------------|---|
| 1 | <code>outd</code> | <code>outs</code> | <code>pam running</code> | <code>(out,sdof) Stark data, output file</code> |
| 2 | <code>n</code> | | | <code>(ric) interference terms (y/n)</code> |
| 3 | <code>new data? or help</code> | | | |

where certain variables already assigned are recalled, with the option of modifying them if necessary.

This second phase deals with the hard computational work. The attempts to save computer time and memory have been mainly carried out for this stage. They will appear all along the following presentation. Indeed, this phase includes the three usual steps: reading, processing and writing data that give us a natural way to organize this section.

3.4.1. *Pam : Data Reading and Preparation.*

As previously mentioned, `pam` gets data from both `samfld.dat` and `miscel..samfld.dat` embodies the sampled microfield distribution probability and `miscel.` holds the plasma conditions with a few other miscellaneous coefficients and the relevant atomic data arranged in one or more blocks. The code reads and successively processes the blocks, that is, the different atomic systems step by step. For a given block, a few preliminary calculations must be performed which are, the filling of the dipole operators, the research of the symmetry properties of the evolution operator and the evaluation of the electron-impact collision operator. The electric dipole matrix element is related to the reduced matrix element by the well-known expression³³:

$$(33) \quad \langle \gamma JM | d_\alpha | \gamma' J' M' \rangle = (-1)^{J-M} \begin{pmatrix} J & 1 & J' \\ -M & \alpha & M' \end{pmatrix} \langle \gamma J \| \mathbf{P}^{(1)} \| \gamma' J' \rangle .$$

These matrix elements are used in three different stages: the radiative dipole elements that connect the ground levels to the excited levels are used for the radiation amplitude calculation, the dipole elements that connect states inside both the ground manifold and the excited manifold are used for the Stark effect evaluation and finally, the whole elements are used for evaluating the collision operator (see appendix B).

The examination of the symmetry properties of the evolution operator is carried out in the routines called `blod` and `blodi` if `ric=y`. This routine finds one relevant permutation which gives to the matrix a block diagonal structure and identifies the blocks that are identical. The following diagonalization will be limited to those blocks that are different from each other and thus is considerably speeded up.

3.4.2. *Pam: Data Processing.*

The first part of this step is simply a sequence of linear algebra operations involving diagonalizations of complex symmetric matrices, matrix inversions and evaluations of scalar products. It is greatly dependent on the scientific library routine used.

³³R. D. Cowan, *The Theory of Atomic Structure and Spectra*, (University of California Press Berkeley CA, 1981).

As already explained, the relevant complex coefficients for the Stark components are picked up at the end of the process from expression (30) and stored into files for further processing.

3.4.3. Pam: Writing.

At the end of the whole process, the complex coefficients are written down into the file `outd`, which will be read and processed by `poum`. An example of such a file is given below. The four first columns hold respectively frequency, real amplitude, imaginary amplitude and width of the individual components. The last column contains a label linking each Stark component to the original radiative transition, for the purposes of certain post-processing algorithms such as FFM or redistribution function calculation.

| | outd | | | | |
|----|-------------|----------------|----------------|----------|---|
| 1 | 3318.132324 | 0.1658917E-07 | 0.5967411E-08 | 0.477309 | 1 |
| 2 | 3318.440186 | -0.2275274E-08 | -0.5980132E-08 | 0.717934 | 1 |
| 3 | 3323.072754 | 0.1079465E-09 | 0.1272007E-10 | 0.321601 | 1 |
| 4 | 3318.132324 | 0.3005932E-07 | 0.1421770E-07 | 0.477309 | 1 |
| 5 | 3318.440186 | -0.1108864E-08 | -0.1420526E-07 | 0.717934 | 1 |
| 6 | 3323.072754 | -0.1067623E-09 | -0.1243583E-10 | 0.321601 | 1 |
| 7 | 3323.036377 | 0.2170943E-07 | 0.000000 | 0.317204 | 2 |
| 8 | 3323.036377 | 0.2170943E-07 | 0.000000 | 0.317204 | 2 |
| 9 | 3318.132324 | 0.1024032E-08 | -0.8536560E-09 | 0.477309 | 2 |
| 10 | 3318.440186 | -0.9122293E-09 | 0.8942456E-09 | 0.717934 | 2 |
| 11 | 3323.072754 | 0.2883410E-07 | -0.4058954E-10 | 0.321601 | 2 |
| 12 | ... | | | | |

3.5. Poum: Data Post-processing : Phase 3.

This phase is the simplest one. Its main function is to prepare data of the kind above into files for graphic applications. Indeed, some of the tasks performed by `poum` could be performed by most of these graphic applications. To monitor the process which customizes the outgoing profiles, an interactive dialog with the code takes place. Its format is nearly the same as the one used by `pim`. The monitoring data can be modified typing, without space character: `variable name=new parameter`.

Moreover, compact but complete information, as shown below, about the different parameters, appears on the screen. It allows casual users to work easily.

| | poum running | |
|---|-------------------|---|
| 1 | outd | outs (out,sdof) Stark comp. data, output file |
| 2 | e | 300 (units,npt)(e/a)eV or A/curve point numb. |
| 3 | 3300.00 | 3340.00 (ai,af) default frequency range |
| 4 | n | f (dop,cv)doppler(y/n)-convl(f)fft(v)voigt |
| 5 | 0.00000 | 0.00000 (wg,wl) Gauss FWHM/ Lorentz HWHM eV |
| 6 | n | (nyn) profile normalization (y/n) |
| 7 | 0.00000 | (shft) shift in output units |
| 8 | new data? or help | |

sdof: output filenames for static (s_s dof), dynamic (d_s dof) lineshapes

units: units=e \rightarrow eV, units=a \rightarrow angstrom

npt: number of data points for s_s dof and d_s dof

a_i, a_f: non zero values are used as new bounds for the profile by the code, otherwise, the bounds found in the input file header are held.

dop: option for Doppler broadening

cv: option for convolution of profiles with Gaussians for Doppler or apparatus function broadening. **cv=f** means that a **fft** algorithm will be used. **cv=v** orders the code to use Voigt profiles instead of Lorentzians.

w_g, w_l: additional apparatus broadening Gaussian or Lorentzian.

nyn: optional normalization of the outgoing lineshape. This can be useful for comparisons performed on isolated lines.

shft: possible shift for the whole profile.

It is during this phase that the FFM is applied.

At the end of execution, **poum** writes the files **s_s dof** and **d_s dof** with the two columns intensity versus energy (or wavelength) with **npt** values of energy (or wavelength).

APPENDIX A. BRIEF LIOUVILLE SPACE REVIEW

Liouville space has been designed to transform expressions such as:

$$(A0) \quad \{e^{iHt} A e^{-iHt}\}_{av'} \text{ into } \{e^{iLt}\}_{av} A.$$

This disentangles the evolution operator averaged over some stochastic process and any observable A .

The Liouville space \mathbf{L} is defined as $\mathbf{H} \otimes \mathbf{H}^d$, the tensorial product of the Hilbert space \mathbf{H} with its dual. The scalar products in \mathbf{H} and \mathbf{H}^d , respectively noted with brackets and parenthesis, are extended to \mathbf{L} with the expression:

$$(A1) \quad \ll \alpha\beta | \gamma\delta \gg = \langle \alpha | \gamma \rangle \cdot (\beta | \delta) = \langle \alpha | \gamma \rangle \cdot \langle \beta | \delta \rangle^*$$

The standard notation $|\alpha\beta \gg$ for Liouville space vectors has been used. It can be seen that:

$$(A2) \quad Tr\{A\} = \sum_f \ll f | A \gg,$$

where $|A \gg = \sum_{\alpha\beta} \langle \alpha | A | \beta \rangle \cdot |\alpha\beta \gg$.

According to (A1) the Liouville "bra" is defined as:

$$\ll A | = \sum_{\alpha\beta} \langle \alpha | A | \beta \rangle^* \cdot \ll \alpha\beta |$$

which gives:

$$(A3) \quad Tr\{AB\} = \ll A | B \gg.$$

The so-called Liouville operators are such that $P|q \gg = |[p, q] \gg$ or

$$(A4) \quad P = p \otimes I^d - I \otimes p^d,$$

where p and q are linear operators in Hilbert space. The Liouvillian based on the type above is generally defined from the Hamiltonian as:

$$(A5) \quad L = \frac{1}{\hbar} (H \otimes I^d - I \otimes H^d).$$

Therefore, its matrix elements in the anti symmetric subspace (built using the ground and the excited manifolds in the no-quenching approximation) are:

$$(A6) \quad \begin{aligned} \ll e_i, g_j | L | e_i, g_j \gg &= \langle e_i | H | e_i \rangle - \langle g_j | H | g_j \rangle^* \\ \ll e_i, g_j | L | e_i, g_k \gg &= \langle g_j | H | g_k \rangle \\ \ll e_i, g_j | L | e_k, g_j \gg &= - \langle e_i | H | e_k \rangle^* \end{aligned}$$

For the present problem it can be seen that:

$$(A7) \quad Tr\{\vec{d} \cdot \vec{d}(t) \rho_0\} = \ll \vec{d} | \cdot \vec{d}(t) \rho_0 \gg$$

which becomes according to (A0):

$$(A8) \quad \ll \vec{d} | U(t) | \cdot \vec{d} \rho_0 \gg$$

with the convention $U(t) = e^{-iLt}$.

APPENDIX B. ELECTRON COLLISION OPERATOR

The relaxation effects on dipoles due to electrons is generally accounted for with an electronic phenomenological collision operator. That means that the electron effect is calculated in the framework of a binary collision impact theory. Then, it is reintroduced (together with the spontaneous relaxation coefficient) in the Liouvillian as an external relaxation mechanism, independent from ions. An element of this operator is written as the sum of three terms³⁴:

$$\begin{aligned}
 \Phi_{\alpha\alpha'\beta\beta'} = & \sum_{\alpha''} \delta_{\beta\beta'} \vec{d}_{\alpha\alpha''} \cdot \vec{d}_{\alpha''\alpha'} G(\Delta\omega_{\alpha''\beta}) \\
 (B1) \quad & + \sum_{\beta''} \delta_{\alpha\alpha'} \vec{d}_{\beta'\beta''} \cdot \vec{d}_{\beta''\beta} G(-\Delta\omega_{\alpha\beta''}) \\
 & - \vec{d}_{\alpha\alpha'} \cdot \vec{d}_{\beta'\beta} [G(\Delta\omega_{\alpha\beta'}) + G(-\Delta\omega_{\alpha'\beta})]
 \end{aligned}$$

with $\Delta\omega_{\alpha\beta} = \omega - \omega_{\alpha\beta}$, where $\omega_{\alpha\beta}$ is the frequency difference between the states α and β . The two first terms are sums over the perturbing states α'' and β'' . If $\alpha = \alpha'$ and $\beta = \beta'$, they are diagonal and they couple a transition $\alpha - \beta$ with itself, they correspond to the atomic scheme shown in Fig. 1(a). The extra-diagonal terms corresponding to the atomic scheme in Fig. 1(b) appear to be negligible. The third term, which is also extra-diagonal, represents the interference effect between the subsets α and β . It couples a transition $\alpha - \beta$ together with a different transition $\alpha' - \beta'$. A schematic representation is given in Fig. 1(c). If these terms are negligible, the collisional operator is diagonal and the interaction operator accounting for the ionic Stark effect in the working subspace $|\alpha\beta\rangle \gg$ is block diagonal, reducing the working matrices and making the final calculation easier. The profile is then a sum of ionic Stark components broadened homogeneously by electrons. When it is impossible to neglect extra-diagonal terms, it becomes impossible to reduce the size of the working matrices and the final calculation can become very cumbersome. In general terms, their effects on the spectral line shape is a reduction of the electronic line width due to the mixing between the involved radiative transitions.

The function $G(\Delta\omega)$ depends on the density n_e and temperature T_e of the plasma and is calculated to second order in the radiation-electron interaction. A thermal average included in $G(\Delta\omega)$ can be performed using a quantum mechanical relaxation theory or a classical path assumption for the perturbing electrons. In the PPP code an expression for $G(\Delta\omega)$ based on a modified semiclassical model is used, in which a strong-collision term C is added to the semiclassical term³⁵:

$$(B2) \quad G(\Delta\omega) = -\frac{4\pi}{3} \left(\frac{2m}{\pi k_B T_e}\right)^{1/2} n_e \left(\frac{\hbar}{m}\right)^2 \left(C + \frac{1}{2} \int_y^\infty e^{-x} \frac{dx}{x}\right)$$

³⁴Earl W. Smith and C. F. Hooper, Phys. Rev. 157, 126 (1967).

³⁵Hans R. Griem, Milan Blaha, and Paul C. Kepple, Phys. Rev. A 19, 2421 (1979).

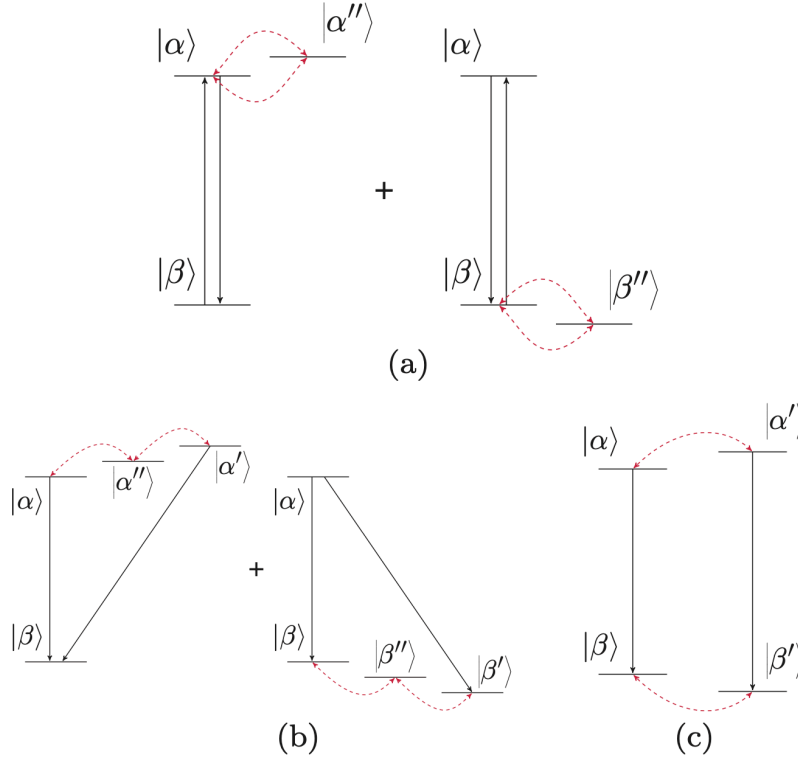


FIGURE 1. Atomic schemes corresponding to (a) diagonal terms of electronic broadening operator, (b) extra-diagonal terms of electronic broadening operator, and (c) interference terms.

where the cutoff y represents the ratio $y = (\frac{\rho_{min}}{\rho_{max}})^2$, ρ_{min} and ρ_{max} being respectively the minimum and the maximum values of the impact parameter range. For non-degenerate systems, the integrand of the thermal average contains oscillating exponentials of the frequency difference. Therefore, ρ_{max} is taken to be the smallest between the Debye radius and a cutoff $v/\Delta\omega_{\alpha\alpha'}$ where v is the mean thermal velocity and $\Delta\omega_{\alpha\alpha'}$ is the frequency difference between the two interacting levels. The minimum value ρ_{min} is a strong collision radius which is the largest of the emitter Bohr radius and the so-called Weisskopf radius ρ_w . The latter quantity is defined by the relation $\frac{V\tau}{\hbar} \approx 1$ where V is the emitter-perturber interaction at distance ρ for the mean interaction time τ . This above behavior has been modeled by the expression:

$$(B3) \quad y = \left(\frac{\hbar n^2}{2z}\right)^2 \frac{\omega^2 + \omega_p^2 + \omega_{\alpha\alpha'}^2}{E_H k_B T}.$$

In this expression, n is the principal quantum number of state α , z is the charge of the ionic core, ω_p is the plasma frequency, and E_H is the ionization energy of atomic hydrogen.

In the neighborhood of the radiated line center ($\Delta\omega = 0$) the impact limit is reached and $G(\Delta\omega)$ tends to the constant value. In the PPP code, the impact-limit expression $G(\Delta\omega = 0)$ has been taken in order to accelerate the lineshape calculations.

In some cases, it is necessary to take into account the omega dependence of G (for neutral hydrogen lines in dense plasmas or high-n lines, or to have the right tendency of the far wings, for example). In such cases, it is possible to calculate the electronic contribution to the total line profile by applying the FFM to electrons alone (using a high-frequency field distribution function and an appropriate mixing rate) and making the convolution of the result with the ion profile calculated without electronic effect.

APPENDIX C. STATIONARY MARKOV PROCESS AND FLUCTUATION RATE.

A finite stationary Markov process is well defined by the static probability of states p_1, p_2, \dots, p_n and a transition rate matrix W , the transition probability matrix P being related to W through

$$(C1) \quad P = e^{-Wt}$$

The particular choice here is defined by:

$$(C2) \quad W_{i,j(i \neq j)} = \nu p_i, W_{i,i} = -\nu(1 - p_i)$$

proportional to the transition rate ν (in the present case, the p_i are the normalized real part of the component intensities). W and p satisfy the required sum rules:

$$(C3) \quad \sum_i W_{i,j} = 0, \sum_j W_{i,j} p_j = 0$$

These expressions define a stationary Markovian process whose associated spectrum is given by:

$$(C4) \quad I(\omega) = \Re \sum_{i,j} (\omega - \Omega + iW + i\gamma)_{i,j}^{-1} (a_i + ic_i)$$

where the elements of the diagonal matrices Ω , and γ are respectively ω_i and γ_i .

The frequency fluctuation rate, ν , manifests the time dependent statistics of the underlying plasma mechanisms which constantly modify the conditions of emission. It could be deduced from observed lineshapes by comparison with both a static and a dynamic model. The two possible ways for the determination of this coefficient are the exponential fitting of simulated field-correlation functions or the use of a model based upon considerations of statistical physics. A simple model was developed and its results compared with simulations performed for weakly coupled plasma conditions. Both agree quite well. Of course, this is limited to cases for which the two time field-correlation function reasonably approaches an exponential. For weakly coupled plasma conditions, the field-correlation function results from three different mechanisms of various relative importance depending on the plasma constituents. A rapid decorrelation behavior due to strong binary collisions takes place for short times. This phase is followed by a slower mid-field decorrelation that dominates the correlation function. For more coupled plasmas, a long time oscillating behavior at the plasma-frequency time scale becomes apparent that guarantees that the time integral of the field correlation function vanishes.

The model used in the present version of the code states simply that field decorrelation is due to binary interactions. This is taken into account in the simple expression that gives the frequency fluctuation rate, ν :

$$(C5) \quad \nu = \frac{v_{th}}{r_s}$$

where $v_{th} = \sqrt{\frac{k_B T}{m_\mu}}$ is the relative mean thermal velocity of ionic perturbors and r_s the ion sphere radius.

Finally, it should be emphasized that the relative variations of the lineshapes, resulting from a variation of the frequency fluctuation rate are weaker. This, results from the general poor sensibility of line shapes to the details of the underlying plasma fluctuations and partly explains why this simple model works so well.